



## SEISMIC RESPONSE CONTROL OF HIGH-RISE BUILDINGS BY USING MTMD WITH LEVER AND PENDULUM MECHANISM

### Akira SONE

Professor, Kyoto Institute of Technology, Japan  
*sone@kit.jp*

### Sunao KATO

Graduate Student, Kyoto Institute of Technology, Japan  
*sunaobaseball@gmail.com*

### Jun SAKAI

Graduate Student, Kyoto Institute of Technology, Japan  
*ynmhh327@yahoo.co.jp*

**ABSTRACT:** In this study, we propose a system to reduce the displacement response of the multiple tuned mass damper (MTMD) that were placed in the roof for seismic response control of high-rise buildings. This is a displacement magnifying mechanism attaching the weight and lever in the horizontal direction in the space between the roof and MTMD, and is so-called Lever and pendulum mechanism(L.D.). In particular, in the paper, the optimum tuning method of the MTMD with L.D. is examined, and by applying the MTMD with L.D. to the single degree of freedom(SDOF) building and the multi-degree of freedom (MDOF) building for response control and, and its effectiveness is examined.

### 1. Introduction

After the 1995 Kobe earthquake has occurred, higher seismic performance is increasingly required in the building, etc.. To satisfy the seismic target performance, research and development for the seismic improvement are actively performed today. Particular, according to the development of seismic technology for supporting the dynamic design, development of high-performance building, the technology of seismic response control has attracted attention from the social background of the safety of building, et al. The technology of seismic response control is to control the responses of high-rise buildings and towers caused by an earthquake or strong wind by using the various mechanisms and devices. For example, the method of installing on the additional mass with damping elements on the building top is relatively used as compact apparatus for easy maintenance. The lever device in this paper is expected to utilize as a vibration control device of the high-rise building. This device is used by adjusting the amount of additional mass and the ratio of the distances between its fulcrum and its power point, and between its fulcrum and its action point, namely a kind of tuned mass damper(TMD).

Also, in the Niigata Chuetsu Earthquake in 2004, long-period ground motion occurred in central area of Tokyo around a distance of about 200km from the epicenter and then accidents of elevators in the high-rise buildings occurred. In The 2011 off the Pacific Coast of Tohoku Earthquake, the elevators and so on of high-rise building in Osaka Prefecture away about 770km from the epicenter were damaged. Furthermore, the sloshing phenomenon for the oil tank occurred due to long-period ground motion in the Niigata East Port, the damage, such as oil leakage came out. In addition, it is pointed out that by the Tokai earthquake, East-Nankai earthquake, et al., long-period earthquake motion will occurs and then the great damages have occurred(Saito, 2010). From this background, in order to apply the lever device to the existing building, the evaluation of earthquake resistance due to long-period ground motion have been studied. The authors et al. have proposed the hybrid TMD using a lever and pendulum mechanism(L.D.)

for controlling the seismic response of MDOF structures, its optimum tuning conditions. Recently, using the high-rise buildings with the TMD using lever device (L.D.) based on the idea of TMD using displacement expansion device and the long-period earthquake motions, its effectiveness of response reduction was examined analytically(Fujinami, 1991),(Yoshimura,1997)

In this paper, using the high-rise buildings with the multiple tuned mass damper (MTMD); that is multiple MTMD using L.D and the long-period earthquake motions, its optimum conditions are shown and its effect of response reduction is examined analytically.

## 2. Analytical Model of High-rise Buildings

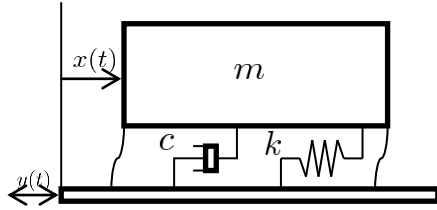


Fig. 1 – SDOF Model

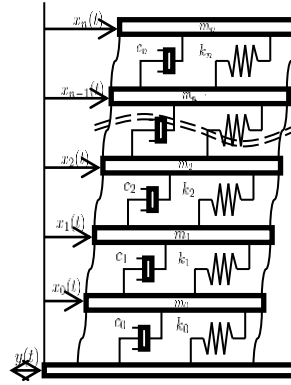


Fig.2 – MDOF Model

Table.1–Rigidity Distribution.

Floor	Rigidity[kN/cm]
10	24500
9	24141
8	23436
7	22377
6	20951
5	19142
4	16923
3	14251
2	11040
1	7067

In this study, as an example of high-rise building, the models of one story building and ten story building are used as shown in Fig. 1 and Fig. 2.  $m$ ,  $c$ ,  $k$  in Fig.1 are mass, damping coefficient and stiffness of building, respectively.  $x$  and  $y$  are the relative displacement of  $m$  and the earthquake ground displacement, respectively.  $m_{i-1}$ ,  $c_i$  and  $k_i$  are mass, damping coefficient and stiffness of  $i$ -th story, respectively. In this study, the fundamental(first) natural period is taken as  $T_1=4.0s$  which corresponds to the natural period of building with 200m in height by tuning for high-rise building or base isolated building. The rigidity distribution of this model is shown in Table 1. Also, mass distribution is uniform distribution, namely;  $m_i=1,249,000kg(i=1,2,3...10)$ .

First, the equation of motion of this system is given by

$$M\{\ddot{x}\} + C\{\dot{x}\} + K\{x\} = -M\{\ddot{y}\} \quad (1)$$

Mass, damping coefficient and stiffness matrices  $M$ ,  $K$  of building model in Fig.2 are given by

$$M = \begin{bmatrix} m_n & 0 & 0 & 0 & 0 \\ 0 & \ddots & 0 & 0 & 0 \\ 0 & 0 & m_2 & 0 & 0 \\ 0 & 0 & 0 & m_1 & 0 \\ 0 & 0 & 0 & 0 & m_0 \end{bmatrix}, \quad K = \begin{bmatrix} k_n & -k_n & 0 & 0 & 0 \\ -k_n & \ddots & \ddots & 0 & 0 \\ 0 & \ddots & k_2 + k_3 & 0 & 0 \\ 0 & 0 & -k_2 & k_1 + k_2 & -k_1 \\ 0 & 0 & 0 & -k_1 & k_0 + k_1 \end{bmatrix} \quad (2)$$

Assuming a stiffness proportional damping, the damping coefficient  $c_i$  of  $i$ -th story is obtained as

$$c_i = \frac{2\zeta_0}{\omega_0} k_i \quad (3)$$

Where,  $\omega_0$  and  $\zeta_0$  are modal circular frequency and modal damping ratio of first mode of building, respectively. Substituting Eq.(3) into stiffness matrix  $K$  in Eq.(2), the damping matrix  $C$  is written as

$$C = \frac{2\zeta_0}{\omega_0} K \quad (4)$$

### 3. Models of High-rise Building with MTMD and Its Optimum Tuning Condition

#### 3.1 Concept of Lever Device)

The concept of dynamic mass is simply described as follows.

(1)The lever device with the tip mass in the space between two slabs separated through the elastic body is mounted as shown in Fig.3. In this figure, blue balls denote the ball bearings.

(2)A two-dimensional relative horizontal displacement  $x$  between the lower and upper slabs becomes the rotational motion of tip mass of lever around fulcrum installed at lower slab.

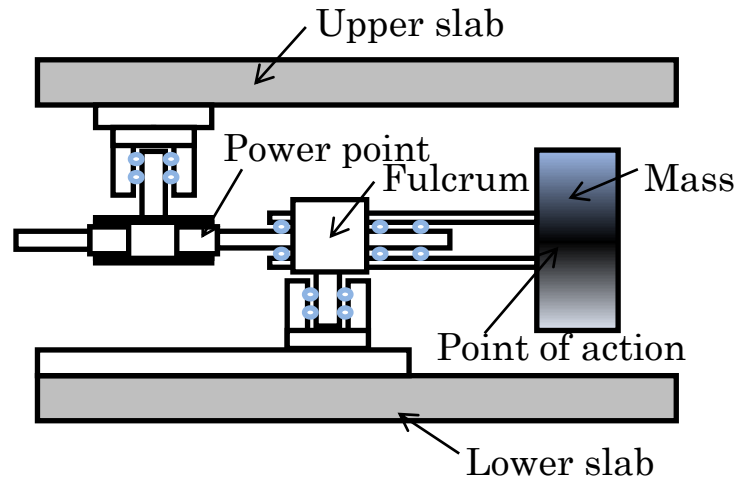


**Fig.3 – Schematic Drawing of Lever Device**

(3)Therefore, at the point of action of lever, the displacement response  $Bx$  increases by lever ratio  $B$ (that is the ratio of distance between the point of action and fulcrum, distance between the power point and fulcrum). Using Two-dimensional relative horizontal acceleration  $\ddot{x}$  and tip mass  $m_p$ , the inertia force  $m_p B \ddot{x}$  occurs.

(4) Multiplying this inertial force by the distance from the tip of the lever to the fulcrum, The resulting bending moment around the fulcrum is obtained as. When this  $m_p B^2 \ddot{x}$  is divided by the distance of the fulcrum and the power point, the couple acting at the power point and fulcrum is obtained. The upper force is used as the response control force of upper slab and lower force acts the lower slab.

In this study, as an example of high-rise building with TMD and a lever device (L.D.), one story building and ten story building are used as shown in Fig. 4 and Fig. 5.  $m_a$ ,  $c_a$ ,  $k_a$  in Fig.4 are mass, damping coefficient and stiffness of TMD, respectively.  $x_a$  are the relative displacement of  $m_a$  from the earthquake ground displacement. In this study, the fundamental (first) natural period is taken as  $T_1=4$  s by tuning for high-rise building or base isolated building. In this study, the lever ratio of lever device is  $B$ .

First, the optimum tuned conditions of the analytical model with a lever device (1.L.D.) in Fig. 4 are obtained by the fixed point method with  $c=0$  and force  $f=F\cos\omega t=Fe^{i\omega t}$  applied to mass  $m$  instead of  $y(t)$ .The equation of motion in Fig. 4 is given by

$$\begin{cases} -m_p B(1+B)\ddot{x} + (m_a + m_p B^2)\ddot{x}_a + c_a(\dot{x}_a - \dot{x}) + k_a(x_a - x) = 0 \\ \{m + m_p(1+B)^2\}\ddot{x} - m_p B(1+B)x_a + kx + c_a(\dot{x} - \dot{x}_a) + k_a(x_a - x_a) = f \end{cases} \quad (5)$$

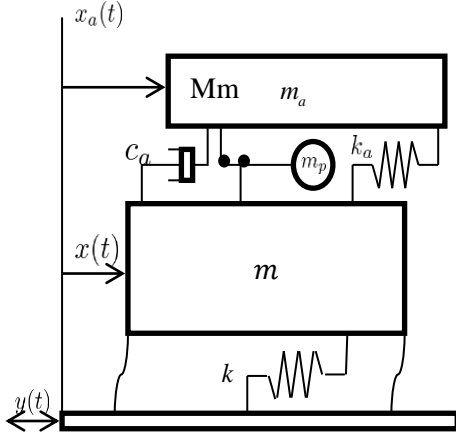


**Fig.4 –Single Degree of Freedom High-rise Model with MTMD and Lever Device**

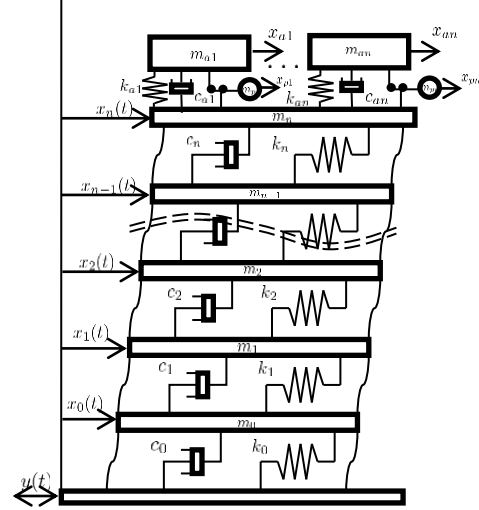


**Fig.5 –Equivalent Shear-spring Structure Model with MTMD and Lever Device**

From these equations with  $x=Xe^{i\omega t}$  and  $x_a=X_a e^{i\omega t}$ , the amplitude ratios  $X/X_{st}$  and  $X_a/X_{st}$  are obtained by

$$\begin{bmatrix} 1 + Av^2 + 2i\mu_1\zeta_a\gamma v & C\mu_1\mu_2v^2 - 2i\mu_1\zeta_a\gamma v - \mu_1\gamma^2 \\ C\mu_2v^2 - 2i\zeta_a\gamma v - \gamma^2 & -Dv^2 + 2i\zeta_a\gamma v + \gamma^2 \end{bmatrix} \begin{Bmatrix} X / X_{st} \\ X_a / X_{st} \end{Bmatrix} = \begin{Bmatrix} 1 \\ 0 \end{Bmatrix} \quad (6)$$

From the above equation, the absolute value of  $X/X_{st}$  is as follows:

$$\left| \frac{X}{X_{st}} \right| = \sqrt{\frac{(\gamma^2 - Dv^2)^2 + (2\zeta_a\gamma v)^2}{\{(AD - C\mu_1\mu_2^2)v^4 + Fv^2 + \gamma^2\}^2 + (2\zeta_a\gamma v)^2 G^2}} \quad (7)$$

The optimum frequency ratio and damping ratio are calculated by

$$\gamma^2 = \frac{AD - C^2\mu_1\mu_2^2}{G}, \quad \zeta_a = \frac{-H - 2D(\gamma^2 - Dv_{P,Q}^2)}{4G\gamma^2 v_{P,Q}^2 \{3Gv_{P,Q}^2 - 4\}} \quad (8)$$

Where

$$\omega_0 = \sqrt{\frac{k}{m}}, \quad \omega_a = \sqrt{\frac{k_a}{m_a}}, \quad \zeta_a = \frac{c_a}{2\sqrt{m_a k_a}}, \quad \mu_1 = \frac{m_a}{m}, \quad \mu_2 = \frac{m_p}{m_a}$$

$$v_{P,Q} = \frac{\omega}{\omega_0} \text{ for points P and Q, } \gamma = \frac{\omega_a}{\omega_0}, \quad X_{st} = \frac{F}{k}$$

$$A = 1 + \mu_1\mu_2(1+B)^2, \quad C = B(1+B), \quad D = 1 + \mu_2B^2$$

$$E = -D - A\gamma^2 - D\mu_1\gamma^2 + 2C\mu_1\mu_2\gamma^2, \quad F = -1 - Av^2 - D\mu_1v^2 + 2C\mu_1\mu_2v^2$$

$$G = A + D\mu_1 - 2C\mu_1\mu_2, \quad H = (-D^2\mu_1 - C^2\mu_1\mu_2^2 + 2CD\mu_1\mu_2)v_{P,Q}^4 \{2(AD - C^2\mu_1\mu_2^2)v_{P,Q}^2 + E\}$$

On the other hand, in the case of multiple TMD with lever device, the optimum tuning condition are not obtained as Eq.(8) by the fixed point theory. Therefore, when installed the  $n$ -number of devices in parallel, it is noticed that the maximum values in Eq.(7) exist at most  $(n+1)$  on resonance curve. When these maximum values are set to  $P_{\max}(1) \sim P_{\max}(n+1)$ , the evaluation function  $J$  for suppressing the resonance peaks and the evaluation function  $I$  to reduce the variation of the peak of the resonance curve by the lever apparatus installation are defined as follows.

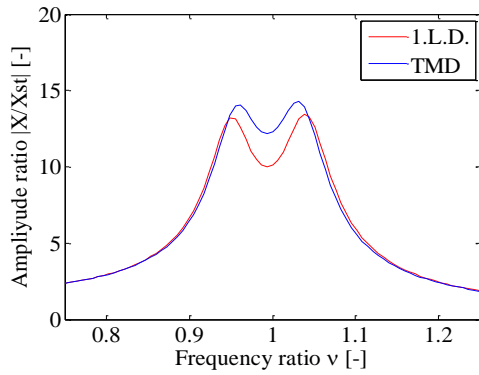


**Fig. 6 – Comparison of Resonance Curves between 1.L.D and TMD**

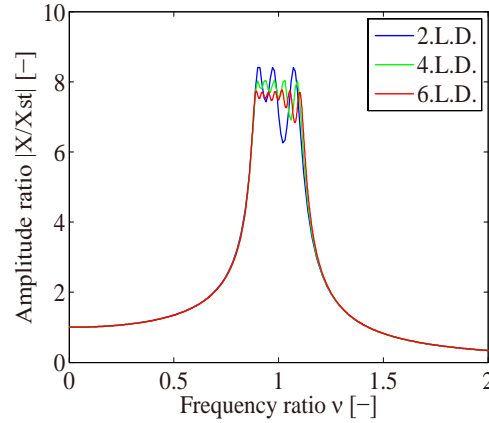


**Fig. 7 – Comparison of Resonance Curves by the Number of Lever Device**

$$I = \sum_{s=1}^{n+1} \left\{ \sum_{r=1}^{n+1} \frac{P_{\max}(r)}{n+1} - P_{\max}(s) \right\}^2, \quad J = \sum_{r=1}^{n+1} \frac{P_{\max}(r)}{n+1} \quad (9)$$

In this study, through the iterative calculation using hill climbing method, the optimum tuning conditions for the frequency ratio  $\gamma$  and damping ratio  $\zeta_a$  are obtained. Figure 6 shows the resonance curves of SDOF structure model with TMD and by TMD with single lever device(1.L.D.). Figure 7 shows the resonance curves of SDOF structure model by MTMD with double lever devices(2.L.D.), quadruple lever devices(4.L.D.) and six double lever devices(6.L.D.). These examples are for the case of mass ratios  $\mu_1=0.01$ ,  $\mu_2=0.1$  and lever ratio  $B=3$ . From these figures, it is shown that the resonance curve using TMD with 1.L.D. is smaller than that of TMD, and its reduction effect is larger with the increase of number of lever device.

## 4. Earthquake Motions for Numerical Simulation

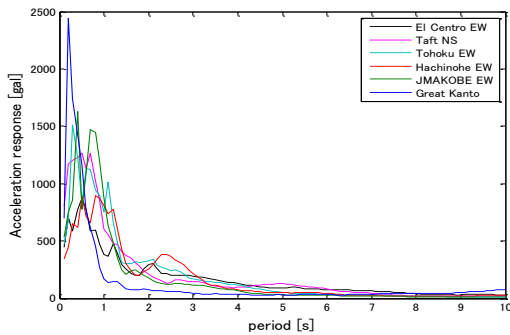
### 4.1. Introduction of Earthquake Motions

In this study, in order to investigate the effectiveness of L.D., as the standard earthquake motion, and as the long-period earthquake motion, the earthquake motions in Table 2 are used. The peak accelerations of these motions are normalized as taking their peak velocity  $V_{\max}=50$  cm/s (The Building Center of Japan, 1986) which is the peak velocity of design earthquake motion (Level=2) for high-rise building without human damages as shown in Table 2 (Aichi Building Housing Center, 2004, Ministry of Construction Building Research Institute Building Center of Japan, 1992, Morioka, Keijo, 1980, Umebayashi, Hiroya, and Kitamura, Haruyuki., 2007). The acceleration, velocity and displacement response spectra obtained by these motions are shown in Figs. 8, 9 and 10, respectively. From the acceleration response spectrum in Fig. 8, it is shown that the standard earthquake motions such as El Centro EW, Tohoku EW, Great Kanto et al. have the short period component of 1 second or less. From Figs. 9 and 10, it is somewhat constant in the all periods, and is contained within a relatively small value. In the seismic isolation structure, by making the fundamental natural period of the structure longer, it is possible to suppress an increase in its response. It can be said, however, if the damping and the stiffness of the structure are too large, there is a risk that causes an increase in acceleration response. As shown in Fig. 8, in the case of long-period earthquake motions such as Nagoya Sannomaru EW, Tonankai Yokohama and Osaka NS, the acceleration response spectrum is smaller than that of the standard earthquake motions. However, from Figs. 9 and 10, the displacement response spectrum and velocity response spectrum are dominated by long-period area of more than 3 seconds. If these high-rise building or base-isolated structures of natural period of 4 seconds or longer period are subjected to the long-period earthquake motions, the concerns about the possibility that an increase in the displacement response occurs are high.

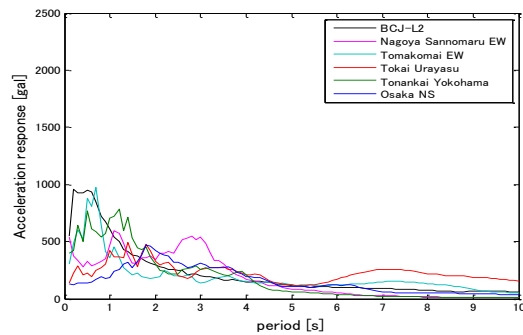
**Table 2 – Earthquake motions for simulation.**

	<b>Earthquake</b>	<b>Maximum acceleration [gal]</b>
<b>Standard earthquake motion</b>	El Centro EW The 1940 Imperial Valley Earthquake(El Centro EW)	292.34
	The 1952 Kern County earthquake (Taft NS)	514.49
	The 1978 Miyagiken-oki Earthquake(Tohoku Earthquake EW),	362.79
	The 1968 Tokachi-oki earthquake(Hachinohe EW)	261.85
	The 199 5Hyougo-ken Nanbu Earthquake (JR Kobe EW)	447.14
	The 1923 Kanto Earthquake(Great Kanto)	630.42
<b>Long-period earthquake motion</b>	The artificial earthquake of Building Center of Japan (BCJ-L2)(1992)	320.97
	Nagoya Sannomaru EW(Aichi Building Housing Center, 2004)	180.31
	The 2003 Tokachi-oki earthquake (Tomakomai EW),	272.96
	Tokai Urayasu, (Umebayasi and Kitamura, 2007)	129.97
	Tonankai Yokohama(Ditto)	290.79
	The 2011 off the Pacific Coast of Tohoku Earthquake(Osaka NS)	121.56

**4.2. Response Spectra of Earthquake Motions**

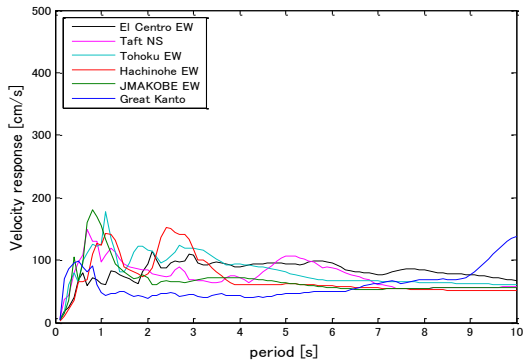


**(a)Standard earthquake motion.**

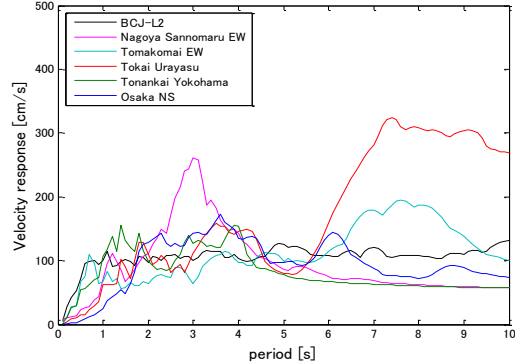


**(b)Long-period earthquake motion.**

**Fig. 8 – Acceleration response spectra.**

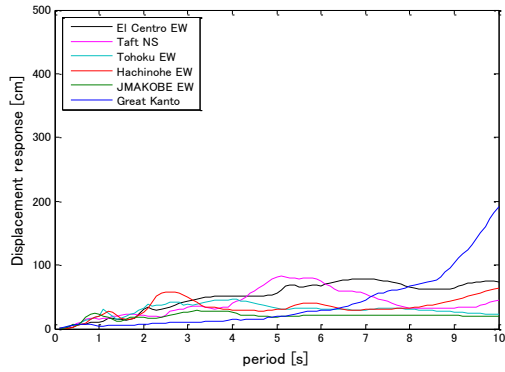


**(a)Standard earthquake motion.**

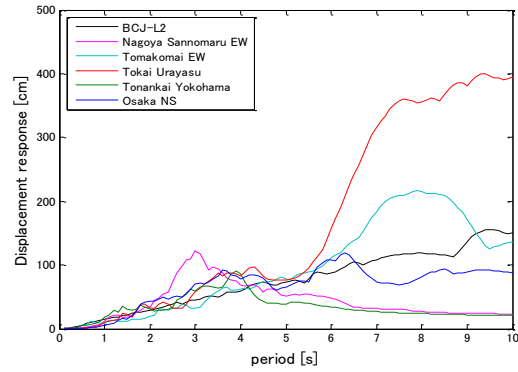


**(b)Long-period earthquake motion.**

**Fig. – 9 Velocity response spectra.**



(a) Standard earthquake motion.



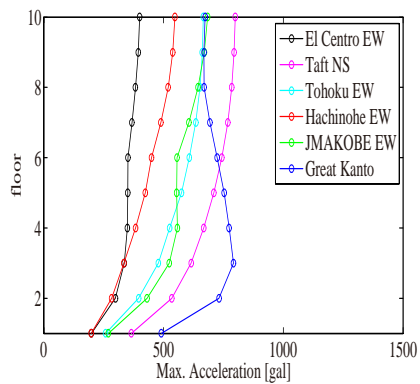
(b) Long-period earthquake motion.

Fig. 10—Displacement response spectra..

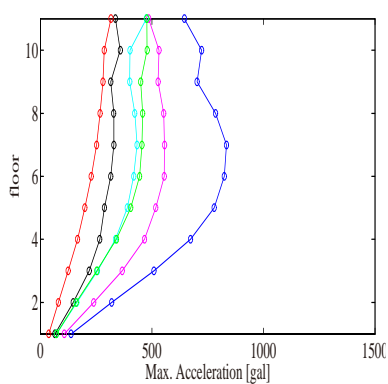
## 5. Simulation Results

### 5.1. Case of MDOF structure model

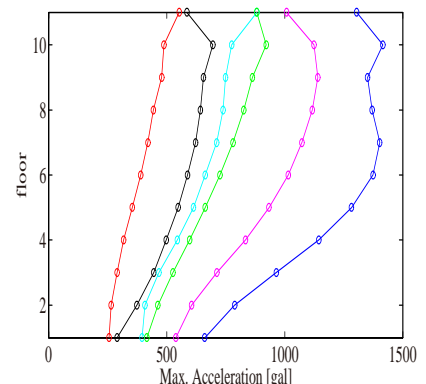
For the MDOF model of high-rise building, using the all above earthquake motions, optimum damping



(a) Without TMD

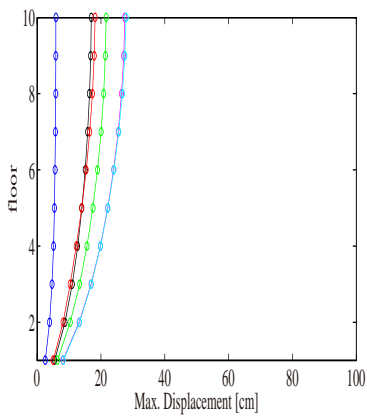


(b) With TMD

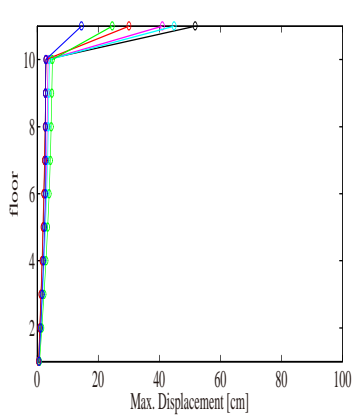


(c) TMD With 4.L.D.

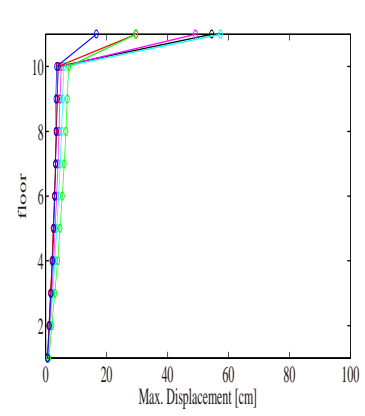
Fig. 11 – Maximum Acceleration of Each Floor (Standard Earthquake Motion)



(a) Without TMD

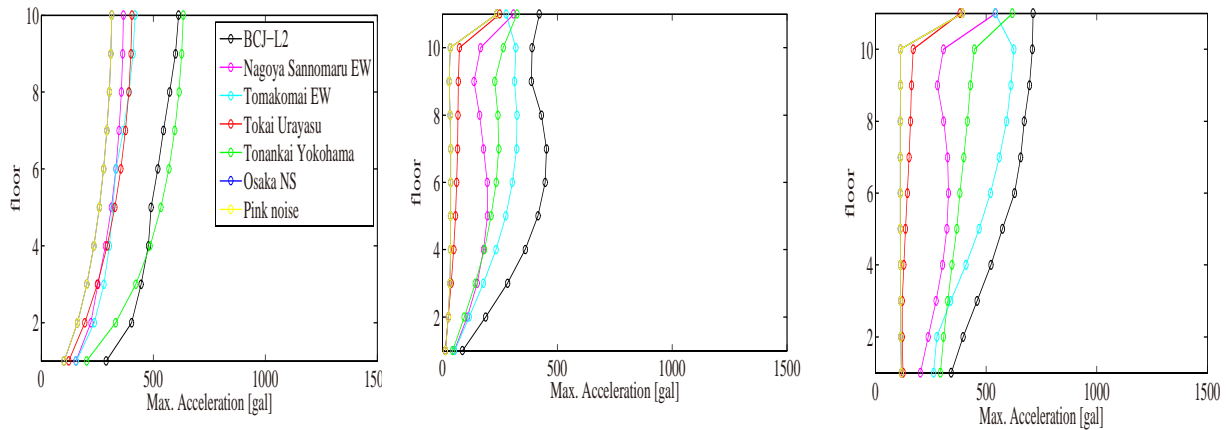


(b) With Only TMD

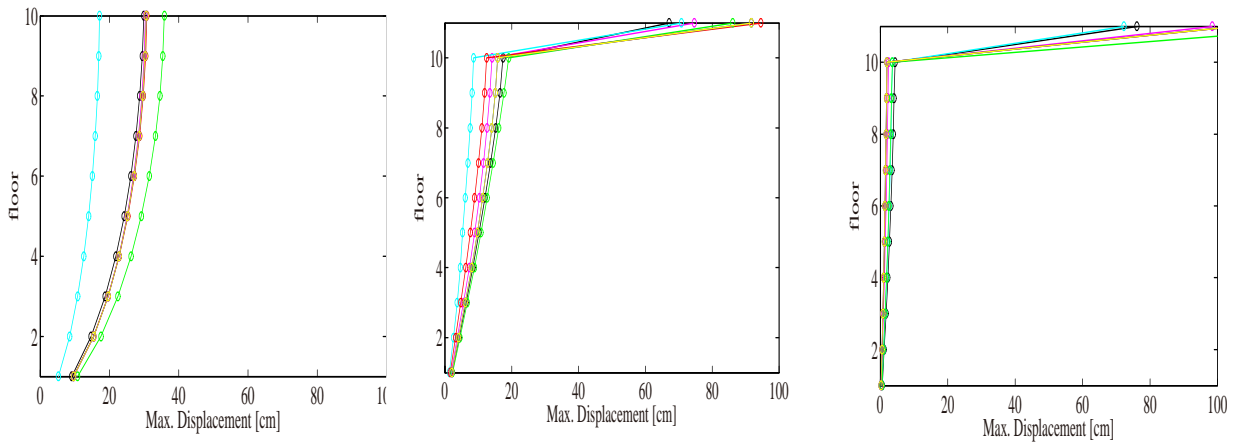


(c) TMD With 4.L.D.

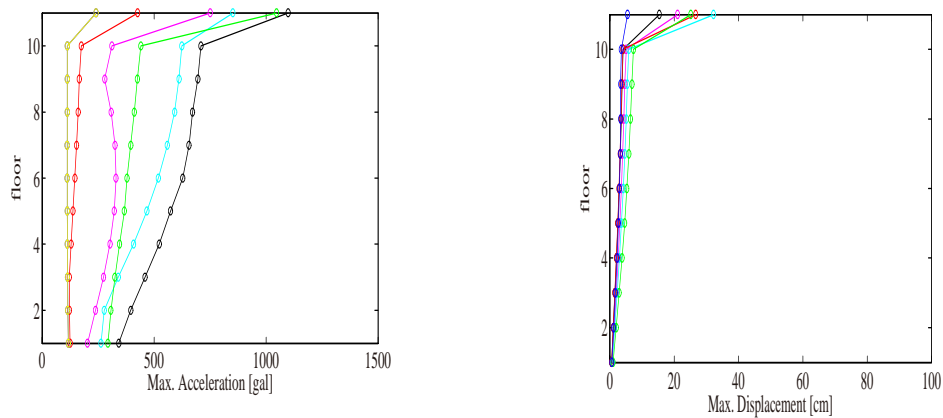
Fig.12 – Maximum Displacement of Each Floor (Standard Earthquake Motion)



(a) Without TMD (b) With Only TMD (c) TMD With 4.L.D.  
**Fig.13 – Maximum Acceleration of Each Floor(Long-period Earthquake Motion)**



(a) Without TMD (b) With Only TMD (c) TMD With 4.L.D.  
**Fig.14 – Maximum Displacement of Each Floor(Long-period Earthquake Motion)**



(a) Maximum Acceleration of Each Floor (b) Maximum Displacement of Each Floor  
**Fig.15 – Maximum Acc. and Disp. of Each Floor with TMD using 1.L.D.(Long-period Earthquake Motion)**



ratio, and lever ratio  $B=3$ , damping ratio of building  $\zeta_0=0.02$  in Eq.(3),  $\mu_1=0.01$ ,  $\mu_2=0.01$ , the maximum acceleration responses and maximum displacement responses of each floor of main mass are shown in Figs.11 -14, respectively. Figures 11 and 12 are for the case of standard earthquake motion. Figures 13 and 14 are for the case of long-period earthquake motion. These figures the comparisons among the cases without TMD.(control-free), with only TMD, and With TMD using 4.L.D., respectively. From Figs.11 and 12, in the case of standard earthquake motion, it is shown that the maximum acceleration responses with TMD using 4.L.D. are larger than those without TMD and with TMD. However, it can be seen that the maximum displacements with TMD using 4.L.D. and TMD become lower than those without TMD, obviously. From Figs.13 and 14, in the case of long-period earthquake motion, it is shown that the maximum acceleration responses almost are same, irrespective of control device. However, it can be seen that the maximum displacements with TMD using 4.L.D. become lower than those with TMD and without TMD. For the comparison of maximum responses by the number of lever device, the example of maximum responses with TMD using 1.L.D. subjected to the long-period earthquake motion is shown in Fig. 15. From Figs. 13,14 and 15, it is clear that the maximum responses of the building by the number of devices are almost same. Also, the maximum acceleration of the TMD tends to increase as the number of devices increases. On the other hand, the maximum displacement of TMD decreases as the number of devices increases. In particular, in the case of Tonankai Yokohama motion which is a long-period ground motion, the maximum displacement of TMD decreases by less than half. From these results, it can be seen that for the long-period ground motion, lever device is effective in reducing the maximum displacement of the building and TMD when the number of lever devices is small. However, the maximum acceleration response of each floor has a similar changes and when the lever device is installed, the maximum acceleration increases more than twice compared with the case of standard earthquake motion. The effect of parameters of device, such as analysis and other conditions of the TMD and L.D. on the maximum response must be considered in the future.

## 6. Conclusions

In this study, in order to reduce the seismic response of high-rise building, the numerical simulations are carried out using the mechanical model of lever device (L.D.). The main results are summarized as follows:

(1)Using the tuned mass damper (TMD) with the lever device for SDOF system subjected to the long-period ground motion, the maximum values of the displacement response and acceleration response of SDOF system have been slightly increased as compared to those with TMD. It is clear that the acceleration response of the mass damper reduces and its displacement responses become smaller than those of TMD such as resonance curves in Figs.6 and 7..

(2)In the MDOF system, the maximum acceleration and the maximum displacement of each floor with TMD using L.D. are compared with those without and with TMD. It is shown that the maximum displacement with TMD using L.D. becomes small slightly. However, for the case of the standard earthquake motions, effectiveness of L.D. is not shown. In the future, we intend to consider this problem and the problem of seismic response control of high-rise building with TMD using L.D. having damping element.

## 7. Acknowledgements

The authors are kindly provided the digital data of Kanto Earthquake. from the Research Institute for Science and Engineering, Waseda University, and the data observed by the strong motion observation network(K-NET) of National Institute for Earthquake Disaster Prevention in preparing this paper. Also, they wish to thank Drs. S. Yamamoto, M. Yamada of Waseda University and T. Nakamura of Obayashi Co. for their helpful advice and idea.

## 8. References

Aichi Building Housing Center, "Creating a Foundation of Ground Motion for Seismic Retrofitting that Takes Into Account the Regional Characteristics in Sannomaru-ku, Nagoya (Summary Version) "

- (in Japanese), 2004, pp.1-79.
- Fujinami,Kengo. et al., "Dynamic Absorber Using the Lever and Pendulum Mechanism for Vibration Control of Structures(The Method of Deciding Parameters for the System)" (in Japanese), *Transactions of the Japan Society of Mechanical Engineers*, Vol.57, No.543, 1991, pp.3490-3496.
- Ministry of Construction Building Research Institute Building Center of Japan, "Technical Guidelines of Input Ground Motion Creating Techniques for Design (draft)" (in Japanese), 1992 's Report of Design Input Ground Motion Research Committee,1992.
- Morioka,Keijo, "The Ground Motion of the Great Kwanto Earthquake of 1923", *Transaction of Architectural Institute of Japan*, No.289, 1980, pp.79-91.
- Saito, Daiki., "Effect of Long-period Earthquake Motion on High-rise Building)" (in Japanese), *Bulletin of Japan Association for Earthquake Engineering*, No. 11, 2010, pp.16-19.
- The Building Center of Japan, " On Ground Motion for Dynamic Analysis of High-rise Buildings"(in Japanese), Building Letter, 1986.
- Umebayashi, Hiroya. and Kitamura, Haruyuki., "Evaluation of Long-period Ground Motion Considering Huge Subduction Earthquake with  $V_E$  and  $S_V$  Spectrum "(in Japanese), *Reprints of Annual Conference of Architectural Institute of Japan*, Vol.B2, 2007, pp.423-424.
- Yoshimura, Yousuke. et al.,1997, "Response Control of Structures by Using tuned Mass Damper with Lever and Pendulum Mechanism" (in Japanese), *J. Struct. Constr. Eng.*, Japan Architectural Institute, No.491, pp.47-53.